ADVANCED HEALTHCARE MATERIALS
www.advhealthmat.de

A Pharmacokinetic Model of a Tissue Implantable Cortisol Sensor

*Michael A. Lee, Naveed Bakh, Gili Bisker, Emery N. Brown, and Michael S. Strano**

Cortisol is an important glucocorticoid hormone whose biochemistry influences numerous physiological and pathological processes. Moreover, it is a biomarker of interest for a number of conditions, including posttraumatic stress disorder, Cushing's syndrome, Addison's disease, and others. An implantable biosensor capable of real time monitoring of cortisol concentrations in adipose tissue may revolutionize the diagnosis and treatment of these disorders, as well as provide an invaluable research tool. Toward this end, a mathematical model, informed by the physiological literature, is developed to predict dynamic cortisol concentrations in adipose, muscle, and brain tissues, where a significant number of important processes with cortisol occur. The pharmacokinetic model is applied to both a prototypical, healthy male patient and a previously studied Cushing's disease patient. The model can also be used to inform the design of an implantable sensor by optimizing the sensor dissociation constant, apparent delay time, and magnitude of the sensor output versus system dynamics. Measurements from such a sensor would help to determine systemic cortisol levels, providing much needed insight for proper medical treatment for various cortisol-related conditions.

1. Introduction

Cortisol is a glucocorticoid hormone that has a number of important functions. Cortisol mediates glucose metabolism, blood pressure, and immune responses.[1] Cortisol also regulates lipolysis and proteolysis for energy and biosynthesis,[2] and has been implicated in memory processes[3] and wound healing.[4] Cortisol is an important biomarker for posttraumatic stress disorder (PTSD),[5] Cushing's syndrome,[6] Addison's disease,[7] and other conditions. Hence, an implantable biosensor capable of real time monitoring of cortisol concentration would be of significant value for diagnosis and treatment of these disorders, as well as general scientific research. In this work, we develop a mathematical model, informed from physiological measurements, to predict dynamic compartmental cortisol concentrations in the human body.

Produced in the adrenal gland, cortisol enters the bloodstream, where ≈90%–95% of cortisol is bound to corticosteroid binding globulin (CBG) and albumin, while the remaining, physiologically active fraction remains free and can circulate to other tissues. CBG has a dissociation constant of 33×10^{-9} M,[8] while the dissociation constant of albumin is sensitive to environmental conditions. Previously reported values of albumin K_D values at 37 °C vary between 333 and 810 $\times$ 10^{-6} M.[8,9] Like several other endocrine hormones, cortisol demonstrates pulsatile release initiated by the hypothalamic-pituitary-adrenal (HPA) axis.[10] On average, there are 15–21 pulses per day with a duration at half maximum of 16 ± 0.61 min and amplitudes between 0 to 30 μg dL^{-1} min^{-1} depending on the timing during the diurnal cycle.[10,11] Typically, cortisol concentrations peak in the late morning and gradually decrease throughout the day until reaching a minimum between 8 p.m. and 2 a.m.[10,12]

Cortisol and its therapeutic equivalent, hydrocortisone, are also important molecules in a number of medical conditions. In Addison's disease, the adrenal gland produces low levels of cortisol, which causes various symptoms in patients, including hypotension, vomiting, weight loss, anorexia, fatigue, and increased skin pigmentation. The typical treatment for Addison's disease is ingestion of oral hydrocortisone.[7] Conversely, excess cortisol, either through endogenous overproduction or overexposure to exogenous glucocorticoid treatment, also has serious consequences.[6,13] In Cushing's syndrome, high concentrations of cortisol can have several consequences, including muscle weakness, an irregular fat distribution, hypertension, dermatological issues, and higher mortality rates.[14] Other conditions that may be associated with abnormal cortisol levels and production include obesity,[15,16] memory consolidation,[17] chronic and acute stress,[18,19] posttraumatic stress disorder,[5] major depressive disorder,[20] bipolar disorder, and schizophrenia.[21]

Given the central role cortisol plays in numerous physiological and pathological processes, cortisol has been utilized as a biomarker for these conditions, primarily quantified using immunoassays and enzyme-linked fluorescent based assays on serum, saliva, urine, and hair samples. Ultrafiltration,

M. A. Lee, N. Bakh, Dr. G. Bisker, Prof. M. S. Strano
Department of Chemical Engineering
Massachusetts Institute of Technology
77 Massachusetts Avenue, Cambridge
MA 02139, USA
E-mail: strano@mit.edu
Prof. E. N. Brown
Institute for Medical Engineering and Science
Massachusetts Institute of Technology
77 Massachusetts Avenue, Cambridge, MA 02139, USA

DOI: 10.1002/adhm.201600650

equilibrium dialysis, and high performance liquid chromatography-mass spectrometry (HPLC-MS) have also been used to isolate the free fraction of cortisol in salivary and serum measurements.[22,23] However, these methods are not currently available as continuous, real time in vivo assays.[1] To construct a continuous cortisol profile, frequent measurements throughout the day and fitting algorithms are necessary because of the irregular nature of cortisol secretions leading to inter- and intrapersonal variation.[24] Such measurements are labor intensive and require extensive patient compliance. Additionally, although salivary cortisol is useful for noninvasive cortisol measurements compared to other common cortisol sample sources, disturbances to the sleep–wake cycle may occur during sample collections, complicating data interpretation.[25] The more nuanced measurements provided by a continuous, in vivo cortisol sensor would be transformative in the characterization of cortisol dynamics in healthy and unhealthy patients. Additionally, other species have different primary glucocorticoids instead of cortisol, such as corticosterone in amphibians, reptiles, and birds and 1 α-hydroxycorticosterone in sharks and rays.[26] To study the physiological role these glucocorticoids play, measurements of these molecules have been taken, but results have been shown to be influenced by sex, seasonal cycles, and diurnal cycles.[27] Sensors to measure cortisol, as well as these other glucocorticoids, would be a much needed clinical and scientific tool.

Several efforts to measure cortisol continuously have been made. Venugopal et al. reported a microporation device that detects free cortisol in interstitial fluid based on electrochemical impedance spectroscopy.[28] Bhake et al. reported a miniature, wearable automatic sampling device coupled to a microdialysis system that was used to take cortisol samples over 24 h that could later be analyzed by enzyme-linked immunosorbent assay (ELISA).[29] However, these technologies have several drawbacks, including the lack of longevity and the difficulty in making such techniques continuous. Our lab has demonstrated sensor platforms such as gel-encapsulated single wall carbon nanotubes (SWNT), whose near infrared (NIR) fluorescence intensity and wavelength can be engineered to respond to different concentrations of biomolecules.[30] This platform may potentially be extended towards in vivo detection using the tissue transparency window to NIR emission.[31] Recent work from our lab, for example, has successfully demonstrated estradiol,[32] nitric oxide,[33] dopamine,[34] fibrinogen,[35] and glucose sensors.[36] As a starting point for an implantable cortisol sensor, this work seeks to construct a mathematical, dynamic model of cortisol concentrations in the human body, using parameters derived or estimated from physiological measurements. A mathematical model serves to predict local concentrations of cortisol encountered by the sensor, the relationship between these local concentrations and systemic concentrations, and sensor attributes that would enable robust cortisol measurements.

To date, several efforts to model cortisol biodistribution have been advanced. Brown et al. formulated a differential equation model of the infusion of cortisol from the adrenal gland to the bloodstream and its clearance by the liver.[37] Faghih et al. modeled blood cortisol dynamics and the dynamic feedback control between adrenocorticotropic hormone (ACTH) and cortisol in the HPA axis.[10,24] Glantz et al. constructed a compartmental cortisol biodistribution model based on interior and exterior volumes.[38] Smith et al. constructed a model to predict cortisol concentrations in the four most common locations of cortisol sampling: the blood, saliva, urine, and hair.[39] To our knowledge, however, a physiologically based pharmacokinetic model has not been developed that distinguishes individual tissues, an issue important for evaluating a sensor implant. Therefore, using a compartmental approach adopted by Sorensen[40] and later by our own lab[41] to model glucose and insulin pharmacokinetics in the body, we propose a new model that will differentiate cortisol concentrations in the bloodstream, muscle, adipose, and brain.

First, mass transfer principles and previously proposed models of blood cortisol dynamics were used to construct a model to predict transient cortisol profiles in the adipose, muscle, and brain tissues.[8,10,37] Waking cortisol values predicted by the model were then verified against experimental values reported in the literature for healthy patients. Then, the underlying blood cortisol profile was modified to replicate that in a previously studied Cushing's disease patient to predict cortisol values in various tissues. Last, analysis of a theoretical cortisol sensor implanted in the adipose interstitial space was performed. Sensor output values were calculated in both the healthy and Cushing's disease patient. Sensor parameters were tuned to provide a robust sensor response with minimal time lags to enable continuous monitoring in both healthy and diseased patients.

2. Model Development

2.1. Compartmental Description

De novo cortisol synthesis occurs in pulsatile events in the adrenal gland (g) followed by infusion into the blood with first order kinetics. Total cortisol is also eliminated from the blood through first order clearance by the liver. From this blood reservoir (rb), the blood circulates to various parts of the body. In the present model, the muscle (m), adipose (a), and brain (b) compartments have been included. These three compartments are divided into two smaller subcompartments, the capillary bed (c) and the interstitial/intracellular zone (i). The parenthetical items refer to the subscripts on variables and parameters to be described later. Each compartment is assumed to be well-mixed, and the interstitial and intracellular spaces are lumped together as one compartment. In all compartments, cortisol exists in protein-bound and free forms. There is no clear consensus in the literature about whether cortisol uptake into cells is controlled by passive diffusion through the phospholipid bilayer, carriers through the membrane, or a combination of the two, but for simplicity, passive diffusion was assumed to be the dominant mechanism because of the lipid solubility of cortisol.[42–44] **Figure 1** illustrates the model structure, while **Table 1** summarizes the variables.

Because the original models for total blood cortisol levels by Faghih et al. and Brown et al. were formulated without consideration of other compartments, the total blood cortisol level is treated as a reservoir, whose concentration does not depend

DOI: 10.1002/adhm.201600650

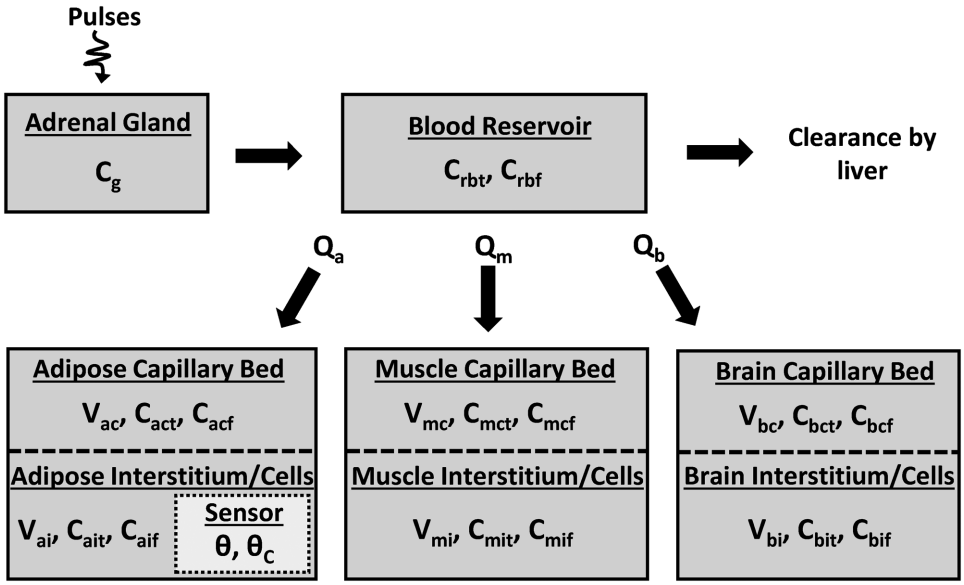

Figure 1. Schematic of model formulation and structure, which represents the body using various compartments with different volumes (V) and cortisol concentrations (C). Cortisol is secreted in pulses in the adrenal gland (g). Cortisol then passes into the blood by first order kinetics. From the blood, cortisol is cleared by the liver. Concentrations in the blood reservoir (rb) serve as the basis to calculate concentrations in the adipose (a), muscle (m), and brain (b). Each of these compartments is divided into the capillary bed (c) and the interstitial/intracellular space (i). In all compartments, cortisol exists in protein bound and unbound forms. Values for total cortisol (t) and free cortisol (f) are calculated. Only the free fraction can travel between the capillary bed and the interstitium. A hydrogel sensor is placed in the adipose interstitial space with cortisol bound sites (θ_C) and unbound (θ) sites.

Table 1. Model variables and parameters.

Variables		Parameters	
C	Cortisol concentration	r	Cortisol source or sink rate
V	Volume	D	Diffusion coefficient
Q	Blood flowrate	L	Sensor thickness
T	Transcapillary diffusion time	θ_T	Sensor binding site concentration
P	Permeability surface area product	K_D	Sensor dissociation constant
θ	Free sensor binding site concentration	k_b	Sensor forward binding rate constant
θ_C	Cortisol bound binding site concentration	β	Sensor output scaling factor
u	Cortisol peak	γ	Cortisol pulse variation scaling factor
q	Cortisol peak amplitude	k_1	Rate constant of cortisol infusion into blood
σ	Cortisol peak amplitude standard deviation	k_2	Rate constant of cortisol clearance by liver
τ	Cortisol peak time	ρ	Compartment density
w	Waiting time between cortisol pulses	K_a	Dissociation constant for albumin–cortisol binding
		K_{cbg}	Dissociation constant for CBG–cortisol binding
		Al	Albumin concentration
		Cbg	Corticosteroid binding globulin concentration
Compartment	First subscript (C, V, T, P, ρ, Al, Cbg, r)	Subcompartment	Second subscript (C, Al, Cbg)
g	Adrenal gland	b	Blood
r	Blood reservoir	c	Capillary bed
a	Adipose	i	Interstitial/intracellular
m	Muscle		
b	Brain		
Cortisol fraction	Third subscript (C)		
t	Total (bound and unbound)		
f	Free fraction		

on interaction with the adipose, muscle, and brain compartments.[10,37] This approximation is justifiable, given that the adrenal gland and liver are the major site of cortisol synthesis and metabolism in the body, the models by Faghih et al. and Brown et al. consider both the adrenal gland and liver, and no external administration of cortisol was considered in this work.[10,37]

Transport of cortisol from the blood to the capillary bed of each compartment occurs by convection. The free fraction of cortisol in the capillary bed can then diffuse into the interstitial compartment with transcapillary diffusion time for compartment k T_k [s], given by

$$T_k = \frac{V_{ki}}{P_k} \tag{1}$$

where P_k [cm^3 s^{-1}] is the permeability surface area product and V_{ki} [cm^3] is the volume of the interstitial subcompartment of compartment k. For the adipose, muscle, and brain compartments, the mass balances for the capillary bed and interstitial space are described by the following equations

$$V_{kc}\frac{dC_{kct}}{dt} = Q_k\left(C_{rbt} - C_{kct}\right) - \frac{V_{ki}}{T_k}\left(C_{kcf} - C_{kif}\right) \tag{2}$$

$$V_{ki}\frac{dC_{kit}}{dt} = \frac{V_{ki}}{T_k}\left(C_{kcf} - C_{kif}\right) + r_k \tag{3}$$

where Q is the volumetric flowrate of blood, C is cortisol concentration, t is time, V is volume, and r is the metabolic cortisol source rate. On each variable, the first subscript refers to compartment k. In the adipose, muscle, and brain, the second subscript (c or i) refers to the capillary or the interstitial subcompartment, while in the blood reservoir, the second subscript (b) refers to blood. The third subscript (t or f) refers to total cortisol or the free fraction of cortisol.

2.2. Pulsatile Events

Pulses of cortisol are introduced to the model based on the method of Brown et al.[37] The waiting time (w) between each pulsatile event is sampled from a gamma distribution with shape parameter α = 54 and inverse scale parameter β = 39, returning values in the unit of hours, which are then converted to the unit of minutes

$$\tau_1 = w_1 \tag{4}$$

$$\tau_i = \tau_{i-1} + w_i \tag{5}$$

where τ_i is the timing of pulsatile event i. The average amplitude of a pulsatile event ($\overline{q}$) is given for $0 \le t \le 1440$ in minutes as

$$\overline{q}(t) = 6.1 - 4.75\cos\left(\frac{2\pi t}{1440}\right) + 3.93\sin\left(\frac{2\pi t}{1440}\right) - 3.76\cos\left(\frac{4\pi t}{1440}\right) - 2.53\cos\left(\frac{4\pi t}{1440}\right) \tag{6}$$

The standard deviation of the average amplitude is

$$\sigma_{\overline{q}}(t) = \gamma\sqrt{\overline{q}(t)} \tag{7}$$

where γ is a coefficient of variation. In this work, γ = 0.1, as was used in the model by Brown et al.[37] The actual amplitude for each pulse was obtained by sampling from a normal distribution with mean $\overline{q}$ and standard deviation σ calculated at that specific time. During the night hours, if a negative amplitude is returned, a pulse amplitude of 1 μg dL^{-1} min^{-1} is used instead.

2.3. Circulation of Cortisol

For the following equations, the initial time point (t = −24 h) corresponds to 12:00 a.m. Because cortisol levels are physiologically low at this time, all of the compartments are assumed to have an initial cortisol concentration of 0 μg dL^{-1}.[10,37] Only values after the first 24 h of simulation are used for further analysis. This allows the stochastic pulses of cortisol to establish an appropriate diurnal cycle for cortisol levels and also eliminates any biases stemming from the 0 μg dL^{-1} cortisol initial condition. The following equations describe the production of cortisol in the adrenal gland, subsequent infusion into the bloodstream, and clearance by the liver

$$\frac{dC_g(t)}{dt} = -k_1 C_g(t) + u(t) \tag{8}$$

$$\frac{dC_{rbt}(t)}{dt} = k_1 C_g(t) - k_2 C_{rbt}(t) \tag{9}$$

$$u(t) = \sum_{i=1}^{N} q_i \delta(t - \tau_i) \tag{10}$$

where k_1 is the infusion rate constant of cortisol from the adrenal glands to the blood, and k_2 is the clearance rate constant of cortisol by the liver, whose values are given in Table S1 in the Supporting Information. The term $u(t)$ is the pulsatile input, and its magnitude q_i is given by sampling from a normal distribution with parameters given by Equations (6) and (7). N is the total number of pulses.

From the blood reservoir, cortisol is carried to the capillary bed of each compartment. From the capillary bed, the free fraction of cortisol diffuses into the interstitial space according to the following equations

$$V_{ac}\frac{dC_{act}}{dt} = Q_a\left(C_{rbt} - C_{act}\right) - \frac{V_{ai}}{T_a}\left(C_{acf} - C_{aif}\right) \tag{11}$$

$$V_{ai}\frac{dC_{ait}}{dt} = \frac{V_{ai}}{T_a}\left(C_{acf} - C_{aif}\right) + r_{ai} \tag{12}$$

$$V_{mc}\frac{dC_{mct}}{dt} = Q_m\left(C_{rbt} - C_{mct}\right) - \frac{V_{mi}}{T_m}\left(C_{mcf} - C_{mif}\right) \tag{13}$$

$$V_{mi}\frac{dC_{mit}}{dt} = \frac{V_{mi}}{T_m}\left(C_{mcf} - C_{mif}\right) \tag{14}$$

Adv. Healthcare Mater. 2016,
DOI: 10.1002/adhm.201600650

$$V_{bc}\frac{dC_{bct}}{dt}=Q_b\left(C_{rbt}-C_{bct}\right)-\frac{V_{bi}}{T_b}\left(C_{bcf}-C_{bif}\right) \quad (15)$$

$$V_{bi}\frac{dC_{bit}}{dt}=\frac{V_{bi}}{T_b}\left(C_{bcf}-C_{bif}\right) \quad (16)$$

$$r_{ai}=\frac{1.5\times10^{-13}\,\text{mol}}{\text{min g tissue}}\rho_{adipose}V_{ai} \quad (17)$$

Note that the adipose interstitial compartment includes a term that describes the conversion of cortisone to cortisol, based on previous experimental measurements.[45] Values for Q_k and V_k were obtained from previously reported values based on a 70 kg man.[40] T_k values were calculated based on experimentally measured mass transfer rates of steroid hormones across membranes and characteristics of tissues.[41,46–50] Methods of calculation are described in detail in the Supporting Information, and Table S2 (Supporting Information) displays parameter values.

2.4. Protein–Cortisol Binding Equilibrium

In all compartments, cortisol exists in both free and protein-bound fractions to either corticosteroid binding globulin or albumin. CBG is the primary binding protein for cortisol with a high affinity, one to one binding stoichiometry but is present in low concentrations. Albumin is an additional binding protein with lower affinity binding with cooperativity effects but is present in higher concentrations.[8] Dorin et al. reported a cubic equation model that considers equilibrium binding to both CBG and albumin, which was used in the present work to determine free and total fractions of cortisol.[8] The solution is reproduced below

$$C_{kjf}=\left(2\sqrt{-\frac{a}{3}}\right)\cos\left(\frac{\phi}{3}\right)-\frac{p}{3} \quad (18)$$

$$a=\frac{3q-p^2}{3} \quad (19)$$

$$b=\frac{2p^3-9pq+27r}{27} \quad (20)$$

$$\phi=\cos^{-1}\left(\frac{-b/2}{\sqrt{-a^3/27}}\right) \quad (21)$$

$$\frac{b^2}{4}+\frac{a^3}{27}<0 \quad (22)$$

$$p=Al_{kj}+Cbg_{kj}-C_{kjt}+K_a+K_{cbg} \quad (23)$$

$$q=Al_{kj}K_{cbg}+Cbg_{kj}K_a-C_{kjt}\left(K_a+K_{cbg}\right)+K_aK_{cbg} \quad (24)$$

$$r=-K_aK_{cbg}C_{kjt} \quad (25)$$

where Al is albumin concentration, Cbg is corticosteroid binding globulin concentration, K_a is the dissociation constant for albumin binding, K_{cbg} is the dissociation constant for corticosteroid binding globulin binding, and subscripts k and j refer to compartments and subcompartments, respectively. Albumin concentrations in the blood, the interstitial fluid of muscle and adipose, and cerebrospinal fluid have previously been measured.[8,51,52] CBG concentrations have also been reported for the blood and cerebrospinal fluid,[8,52] but to the best of our knowledge, no such measurements are reported specifically for CBG in the interstitial fluid of muscle and adipose. As an assumption, the ratio of CBG to albumin in the blood is kept constant in the muscle and adipose tissues and used to calculate protein bound cortisol in the interstitial spaces based on previously measured albumin concentrations in those spaces. The dissociation constants are assumed to remain the same among all the compartments. Parameter values are given in Table S3 in the Supporting Information.

2.5. Sensor Description and Formulation

A hydrogel sensor of a disk shape and thickness L is placed in the interstitial subcompartment of the adipose tissue for the simulations. The thickness of the hydrogel is assumed to be much smaller than its diameter, such that only one spatial dimension must be considered. From the interstitial fluid, free cortisol diffuses into the hydrogel and binds reversibly to sensor binding sites dispersed throughout the gel. The sensor output then changes as a function of the concentration of hydrogel-bound cortisol.

The hydrogel is represented with the transient 1D reaction–diffusion equation

$$\frac{\partial C}{\partial t}=D\frac{\partial^2 C}{\partial x^2}+r_S \quad (26)$$

$$r_S=K_Dk_b\theta_C-k_b\theta_C \quad (27)$$

$$\theta+\theta_C=\theta_T \quad (28)$$

where x describes axial position along the hydrogel, t is time, k_b is the forward rate binding constant to sensor binding sites, K_D is the corresponding dissociation constant, θ is the free binding site concentration, θ_C is the bound cortisol concentration, θ_T is the total binding site concentration, and r_S is the net rate of cortisol unbinding from the hydrogel. The values for k_b and K_D are estimated from the binding properties of cortisol to the glucocorticoid receptor.[53] The partial differential equation was solved using the method of lines, which is described in detail in the Supporting Information. The adipose interstitial cortisol concentration serves as the boundary condition on both ends of the hydrogel. The hydrogel was assumed to contain no cortisol at $t = -24$ h, which is a close approximation of the nighttime condition. The sensor response is assumed to be a turn-off fluorescence sensor with the following mathematical form[32]

$$\text{sensor output} = \frac{\overline{F} - F_0}{F_0} = -\beta \frac{\overline{\theta}_C}{\theta_T} \quad (29)$$

where β is a scaling factor for the sensor response, $\overline{\theta}_C$ is the average bound cortisol concentration within the hydrogel, and θ_T is the total concentration of binding sites. $\overline{F}$ and F_0 are the average fluorescence and original fluorescence of the nanosensors encapsulated within the hydrogel, respectively. The parameter values are listed in Table S4 in the Supporting Information.

2.6. Sensor Optimization

To characterize and optimize the sensor response, sensor design parameters were changed over several orders of magnitude, including the hydrogel thickness (L), the total binding site concentration (θ_T), the forward rate binding constant (k_b), and the dissociation constant (K_D). To extract details about sensor characteristics, a single pulse of 25 μg dL^{-1} was introduced to the adrenal gland and allowed to propagate according to the equations described above. The maximum sensor output was recorded, and the delay time of the peak sensor output value was calculated relative to the peak value in the interstitial adipose compartment.

3. Results and Discussion

3.1. Model Validation

The model was validated by comparing daily peak cortisol values predicted by the model to daily peak values reported in the literature for various compartments in healthy patients (**Table 2**).[10,28,29,52,54–57] The total cortisol levels in the blood correspond well with those measured by Faghih et al. over 24 h.[10] As the cited studies measured free cortisol values in the subcutaneous space and interstitial fluid measurements, those values were compared against free cortisol in the muscle and adipose interstitial concentrations predicted by the model. To the best of our knowledge, there are no studies measuring protein bound cortisol in the adipose and muscle interstitial fluid against which we could validate our calculations. The total cortisol concentration in the brain interstitial concentration in the model was compared to reported measurements in cerebrospinal fluid, as at least one study explicitly mentions measuring both free and protein bound fractions.[52] Not all of the studies shown in Table 2 reported timing of the measurements in relation to the circadian cycle of cortisol, but the waking values predicted by the model agree with the maximums of reported experimental values to an order of magnitude.

Table 2. Comparison of predicted peak cortisol concentrations in compartments to experimental measurements in the literature. Some of the listed studies do not describe the exact timing of cortisol measurements, but the model values generally agree with those reported in the literature. The highest values from each study are compared to daily peak cortisol concentrations calculated by the model. Values from studies are reported either as ranges or confidence intervals based on the original report.

Model compartment	Model value [μg dL^{-1}]	Reported compartment	Study	Reported value [μg dL^{-1}]
Blood	17–27	Blood–total cortisol	Faghih et al.[10]	15–25
Interstitial adipose	1.30–1.89	Interstitial fluid–free cortisol	Venugopal et al.[28]	1.00–1.45
			Cohen et al.[54]	0.1–0.3
			Bhake et al.[29]	0.54–3.62
Interstitial brain	1.07–1.57	Cerebrospinal fluid–total cortisol	Mehta et al.[55]	1.05 ± 0.67
			Holub et al.[56]	0.29–0.43
			Santarsieri et al.[57]	0.45 ± 0.04
			Schwarz and Pohl[52]	0.94 ± 0.18

3.2. Cortisol Dynamics

The cortisol levels for normal patients in the adrenal gland, blood reservoir, adipose tissue, muscle tissue, and brain tissue are shown in **Figure 2**. Cortisol concentrations peak around waking time, which is assumed to be ≈ 8 a.m. in this model. The concentrations of cortisol in all areas are in a physiologically feasible range for normal patients. Note that only data starting from $t = 0$ were used in analyses. For the same representative dataset, **Table 3** compares peak blood free cortisol concentrations and timing to free cortisol concentration and timing in the other compartments. A particular focus was placed on free cortisol because it is the physiologically active fraction.[8] Total cortisol concentration profiles are almost identical between the capillary beds of the various compartments and the blood reservoir because roughly 92%–98% is bound to serum proteins and unavailable for diffusion outside of blood vessels. The ratios of free cortisol in the capillary beds to free cortisol in the blood reservoir are all greater than 0.9. Conversely, the interstitial spaces exhibit much lower total cortisol concentrations than the total blood concentration because only the free fraction of cortisol is available for diffusion into the interstitial space. The adipose and muscle interstitial space peak free cortisol concentrations represent roughly 90% and 80% of the peak free cortisol concentration in the blood, respectively, while that in the brain represents roughly 70%.

Two factors largely determine the transport of cortisol from the blood into the surrounding compartments: the binding equilibrium of cortisol and its proteins and the transcapillary diffusion time. As discussed previously, the binding equilibrium determines the fraction of cortisol that is available for diffusion, while the transcapillary diffusion time characterizes the resistance to diffusion into the surrounding tissues, which in turn affects the peak concentrations and the time delay in each compartment. The muscle and adipose intracellular spaces have identical transcapillary diffusion times and consequently very close transient cortisol profiles, with the differences being the conversion of cortisone to cortisol in the adipose tissue and different concentrations of CBG and albumin. The brain, which has a transcapillary diffusion time that is larger by almost

Adv. Healthcare Mater. 2016,
DOI: 10.1002/adhm.201600650

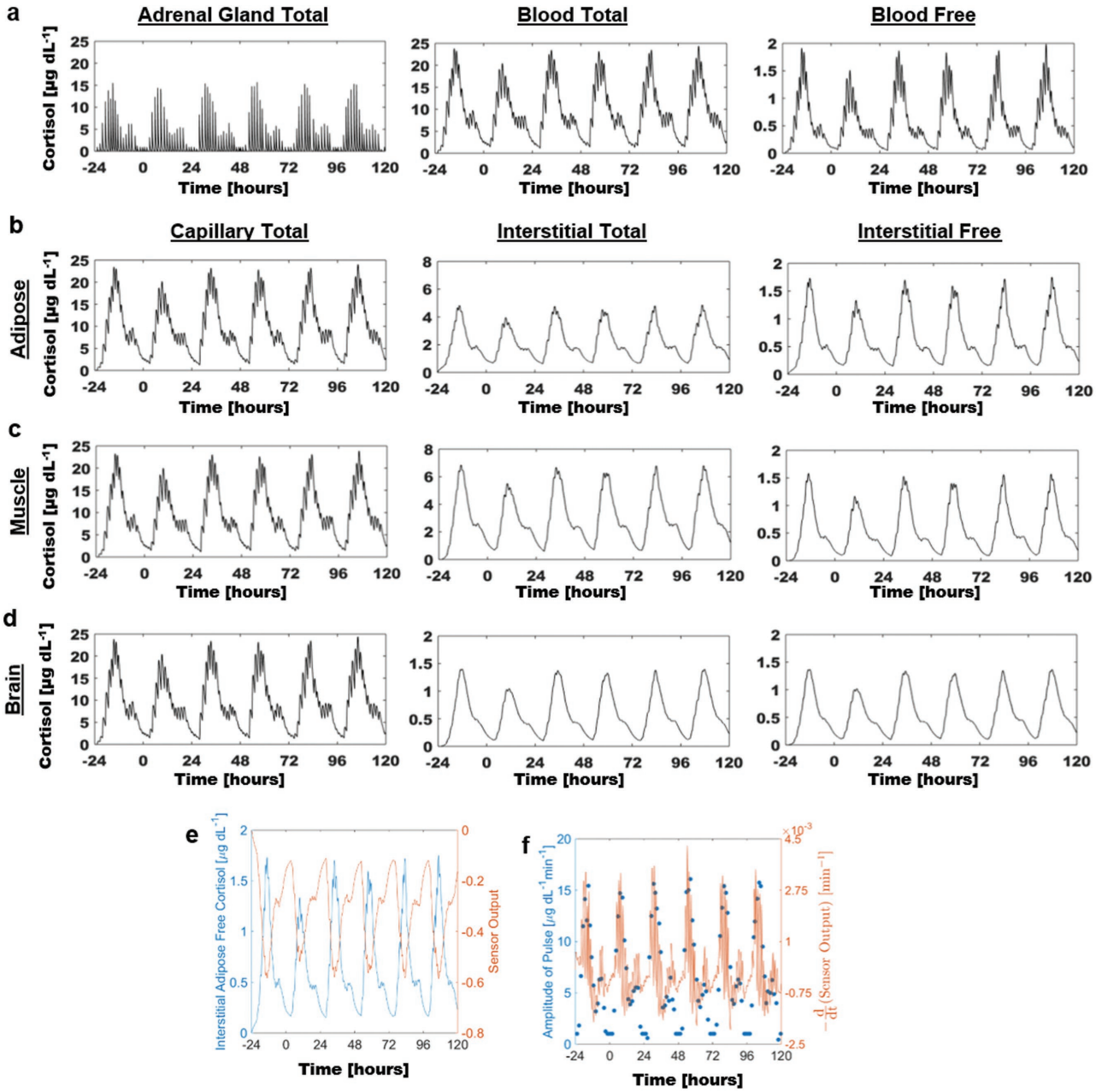

Figure 2. Cortisol concentrations throughout the body as predicted by the model. a) The models by Faghih et al. and Brown et al. were adapted to calculate cortisol levels in the adrenal gland and blood.[10,37] These calculations were then used to calculate total and free cortisol values in the b) adipose tissue, c) muscle tissue, and d) brain tissue. These three compartments were subdivided into the capillary bed and a lumped interstitial/intracellular space. e) Intracellular adipose cortisol concentration (blue) and the sensor output (red). The shape of the sensor output maps the transient cortisol profile. f) Cortisol pulses (blue) and the negative of the derivative of the sensor output (red). There is a correspondence between the number and size of disturbances in the derivative and the number and amplitude of pulses. In this representative data set, only data from $t = 0$ were analyzed to allow the establishment of a proper diurnal cycle and to avoid any slight biases arising from the assumed initial condition of 0 cortisol at 12 a.m. of day −1 ($t = -24$ h).

an order of magnitude compared to the muscle and adipose tissues, possesses several noticeable characteristics because of its longer transcapillary diffusion time: lower peak cortisol concentrations, delay, and smoothing of the cortisol peaks. In the adipose and muscle intracellular compartments, the transcapillary diffusion time is sufficiently small to distinguish individual pulses.

The effects of interstitial protein binding of cortisol were also investigated in more detail. Because each interstitial subcompartment contains different concentrations of CBG and albumin, the proportion of free cortisol relative to the total varies among the compartments. Within a compartment, however, interstitial protein binding has some small effects on the timing and magnitude of peak cortisol values (Figure S1,

Table 3. Comparison of peak free cortisol concentrations and time delays in compartments relative to those in the blood. The time delay is defined as the difference in time between the cortisol peak in the blood and the cortisol peak in the compartment.

Compartment	Ratio to free peak	Time delay of peak [min]
Blood	1	0
Adipose capillary	0.95	3
Adipose intracellular	0.90	35
Muscle capillary	0.93	3
Muscle intracellular	0.80	40
Brain capillary	0.93	1
Brain intracellular	0.70	70
Sensor output		40

Supporting Information). When interstitial protein concentrations are set to 0 for an identical set of cortisol pulses, free cortisol peaks in the adipose interstitial space occur roughly 10 min earlier and are more pronounced. The presence of interstitial protein binding dampens cortisol pulses. However, since the mass transfer driving forces described in Equations (11)–(16) are based on free cortisol values, the difference in peak values is relatively small at less than 10%. In other words, larger variations in free cortisol concentration result from the stochastic pulsatile input in the adrenal gland compared to the inclusion of interstitial protein binding.

Differences in the cortisol profile between compartments have significant implications for the placement of the sensor. Using the parameters listed in Table S4 (Supporting Information), the sensor itself has roughly a 5 min time lag compared to its compartment and a decreased cortisol concentration due to transport barriers. As such, the sensor should be placed in a location with minimal time lag itself. Additionally, the sensitivity of the tissue to each pulse of cortisol is important if the sensor is to be used to correlate local cortisol concentrations with systemic cortisol concentrations. With these considerations in mind, further analyses of the hypothetical sensor were performed under the assumption of implantation in the adipose interstitial compartment, which showed sufficient sensitivity in distinguishing individual peaks of cortisol, as well as smaller time delays relative to the muscle and brain. The adipose is also likely the most accessible region of implantation and signal measurement. In order to obtain an approximate time scale of adipose tissue clearance of cortisol, an exponential curve was fit to the transient cortisol profile in the adipose tissue compartment following a single pulse of cortisol of 25 μg dL^{-1}, as shown in Figure S2 (Supporting Information). The profile was fit to the following form

$$C = C_0 e^{-\frac{t}{\tau_{tissue}}} \tag{30}$$

$$\tau_{tissue} = 140 \text{min} \tag{31}$$

This fit approximates cortisol clearance as a first order kinetic process in order to calculate τ_{tissue}, a characteristic time of adipose tissue clearance.

3.3. Sensor Response

The hypothetical sensor is modeled by considering a prototypical SWNT sensor used by our group. As in the model by Bisker et al. for an implantable insulin sensor,[41] the total concentration of binding sites was calculated by assuming a hydrogel concentration of 10 mg L^{-1} of SWNTs, an individual SWNT length of 1 μm, and binding site separation of 50 nm. This leads to an overall SWNT binding site concentration of 200×10^{-9} M. The rate constant for cortisol binding (k_b) and dissociation constant (K_D) for the SWNT constructs – 0.01×10^{-9} M^{-1} min^{-1} and 34×10^{-9} M, respectively – were estimated by comparison to previously reported values for a model of cortisol binding to glucocorticoid binding receptor.[53] Although SWNT sensors are used as the basis of this calculation, the model is equally applicable to other sensors whose binding site concentrations and kinetic parameters are known. The hydrogel was assumed to have a thickness of 0.5 mm, and the diffusion coefficient of cortisol within the gel (D) was estimated as 3×10^{-10} m^2 s^{-1}.[58] The characteristic times of diffusion (τ_D), binding (τ_b), and unbinding (τ_u) can then be calculated in the following way

$$\tau_D = \frac{L^2}{D} = 13.9 \text{ min} \tag{32}$$

$$\tau_b = \frac{1}{k_b \theta_T} = 0.5 \text{ min} \tag{33}$$

$$\tau_u = \frac{1}{k_b K_D} = 2.94 \text{ min} \tag{34}$$

Because τ_{tissue} is greater than τ_D, τ_b, and τ_u, the encapsulation of the sensor and the binding kinetics do not limit the sensor response, as the dynamics of the sensor–cortisol interactions are faster than cortisol dynamics in the adipose tissue.

In order to visualize in vivo cortisol dynamics with the finest detail, the sensor should be placed in a location that preserves the cortisol profile. Figure 2e shows a representative interstitial adipose cortisol profile and the corresponding sensor response. Because the sensor response resembles the underlying profile of its compartment, sensor placement is critical. Thus, placing the sensor in the adipose or the muscle as opposed to the brain allows for more fine information to be extracted, which can then be used to correlate to the blood levels for a sense of the systemic cortisol levels.

Tracking the cortisol concentration over a period of days yields valuable information about baseline cortisol values at different times of day, which may inform medical treatment for people with various conditions such as PTSD.[5,59] Additionally, due to the pulsatile nature of cortisol release, the derivative of the sensor output allows clearer visualization of the number of pulses occurring within a time interval. Figure 2f shows the negative of the derivative of the sensor response over a period of 5 d. The derivative can directly inform the user about the frequency and amplitude of the pulses throughout the day. Information about the frequency of pulses can inform sensor users about possible issues of hyposensitivity to stress, hypersensitivity to stress, unusual exposures to stress, and other similar

issues. Altogether, with the information of the frequency and amplitude of the pulses from the derivative and information about baseline values from the actual response, a comprehensive picture of the underlying transient cortisol profile can be pieced together, making a continuous cortisol sensor valuable.

3.4. Application of Model to Cushing's Disease Patient

Previous studies have measured 24 h blood cortisol profiles in patients with excess cortisol concentrations. Linkowski et al. measured higher cortisol concentrations in patients with major depressive illnesses and attributed hypercortisolism to higher cortisol pulses amplitudes.[60] In another study, van den Berg et al. detected higher cortisol pulse amplitude and frequency in patients suffering from Cushing's disease.[61] As a model case, we simulated cortisol pharmacokinetics based on the blood cortisol levels of the male Cushing's disease patient studied in the van den Berg experiments. This patient has blood cortisol levels between 50 and 100 μg dL^{-1} with no obvious diurnal pattern. To obtain the same general pattern of total blood cortisol, pulses of 38 ± 2.5 μg dL^{-1} min^{-1} with a 59 ± 11 min waiting time between pulses were introduced into the pharmacokinetic model. Again, initial conditions of 0 μg dL^{-1} cortisol were used in all compartments. The total blood cortisol concentrations resembled that of the van den Berg patient, and the corresponding compartmental concentrations, as well as theoretical sensor output, were calculated (**Figure 3**).

The data show several distinctive features of Cushing's disease patients. Patients with hypercortisolism exhibiting this particular blood cortisol profile have adipose, muscle, and brain interstitial space free cortisol concentrations that are commensurate with total blood cortisol concentrations in healthy patients, as well as a higher proportion of free cortisol concentrations in the blood. The lack of a diurnal cycle also allows the cortisol concentrations in the interstitial adipose, muscle, and brain compartments to be roughly equal, as time delays no longer prevent the brain interstitial space from reaching the same cortisol concentrations as the adipose and muscle. Additionally, using the parameters given by Table S4 (Supporting Information), the theoretical sensor exhibits an output that falls within a much narrower range than that in the healthy patient and is almost saturated, showing the utility of an affinity based sensor in distinguishing between healthy and Cushing's disease patients and indicating the need for appropriate sensor design to avoid sensor output saturation. To predict biodistribution of cortisol in other types of disorders and determine necessary sensor parameters for continuous monitoring, this model may be extended by introducing appropriate patterns of cortisol secretory events.

3.5. Sensor Optimization

In order to characterize an ideal continuous cortisol sensor, four parameters were varied individually to see the effect on the maximal sensor response and the time delay of the response. These parameters include the sensor thickness, the forward binding constant, the dissociation constant, and the concentration of binding sites within the hydrogel implant (**Figure 4**).

The maximal sensor response and the time delay are largely invariant over four orders of magnitude of sensor binding site concentration from 10^{-10} to 10^{-7} M (Figure 4a). However, both the time delay and the maximal response decreased with increasing concentration of binding sites, presumably a consequence of roughly the same level of cortisol reacting with what represents a smaller fraction of the total population of binding sites. The maximum output decreased from 50% to 20%, while the time delay increased from 3 to 105 min. Given the concentration of free cortisol in the adipose tissue ($\approx 50 \times 10^{-9}$ M in healthy patients according to the model), a low concentration of binding sites renders the sensor more sensitive to changes in cortisol concentration. Additionally, lower concentrations of binding sites would be easier to achieve in practice, as sensor material could simply be diluted to the appropriate values. However, using an excessively low concentration of sensor binding sites may result in sensor output saturation, as was almost the case in the model Cushing's disease patient.

The sensor thickness was varied from 0.4 mm to 1 cm (Figure 4b). The maximum output decreased from 40% to 7%, while the time delay increased from 5 to 122 min. Overall, the sensor was more sensitive and robust with smaller dimensions, but in practice, a larger sensor thickness is easier to construct and less subject to noise in the measurements.[41] A balance, therefore, would have to be achieved. A 1 mm thickness offers a time delay of roughly 24 min, which provides enough responsivity to distinguish individual cortisol pulses. Using thinner thicknesses, however, reduces diffusional barriers to increase sensor responsivity.

Increasing k_b from 10^3 to 10^8 M^{-1} min^{-1} while keeping K_D constant increases the maximal output from 0% to 40% and decreases the time delay from 640 to 5 min (Figure 4c). Increasing K_D from 10^{-10} to 10^{-4} M while keeping k_b constant decreases the delay time but also reduces the maximum response from 100% to 0% (Figure 4d). Both extremes represent nearly irreversible binding and no binding at all, respectively. To accurately monitor increases and decreases of cortisol concentration throughout the diurnal cycle, the sensor should exhibit neither extreme.

From this analysis, then, we propose constructing a sensor with the following design. Sensors should have roughly 1 mm or lower thickness, a dissociation constant of 100×10^{-9} M, and a binding site concentration with the value of 200×10^{-9} M, such that cortisol can readily bind and unbind sensor sites to induce changes in sensor output. When sensor output is linearly dependent on the fractional binding site coverage, as was assumed in Equation (29), the binding site concentration should lie close but higher than the dynamic cortisol concentrations encountered in the implantation site in vivo. In the case of the Cushing's disease patient examined in this study, a θ_T value of 200×10^{-9} M allows the sensor to provide an unsaturated output, while still being able to provide a range of outputs reflecting the diurnal cycle of cortisol in a normal patient. The kinetics of binding and unbinding necessitate that K_D and θ_T have values of the same order of magnitude. As can be calculated by Equations (32)–(34), a design with such K_D and θ_T allows the characteristic time of binding and unbinding to be

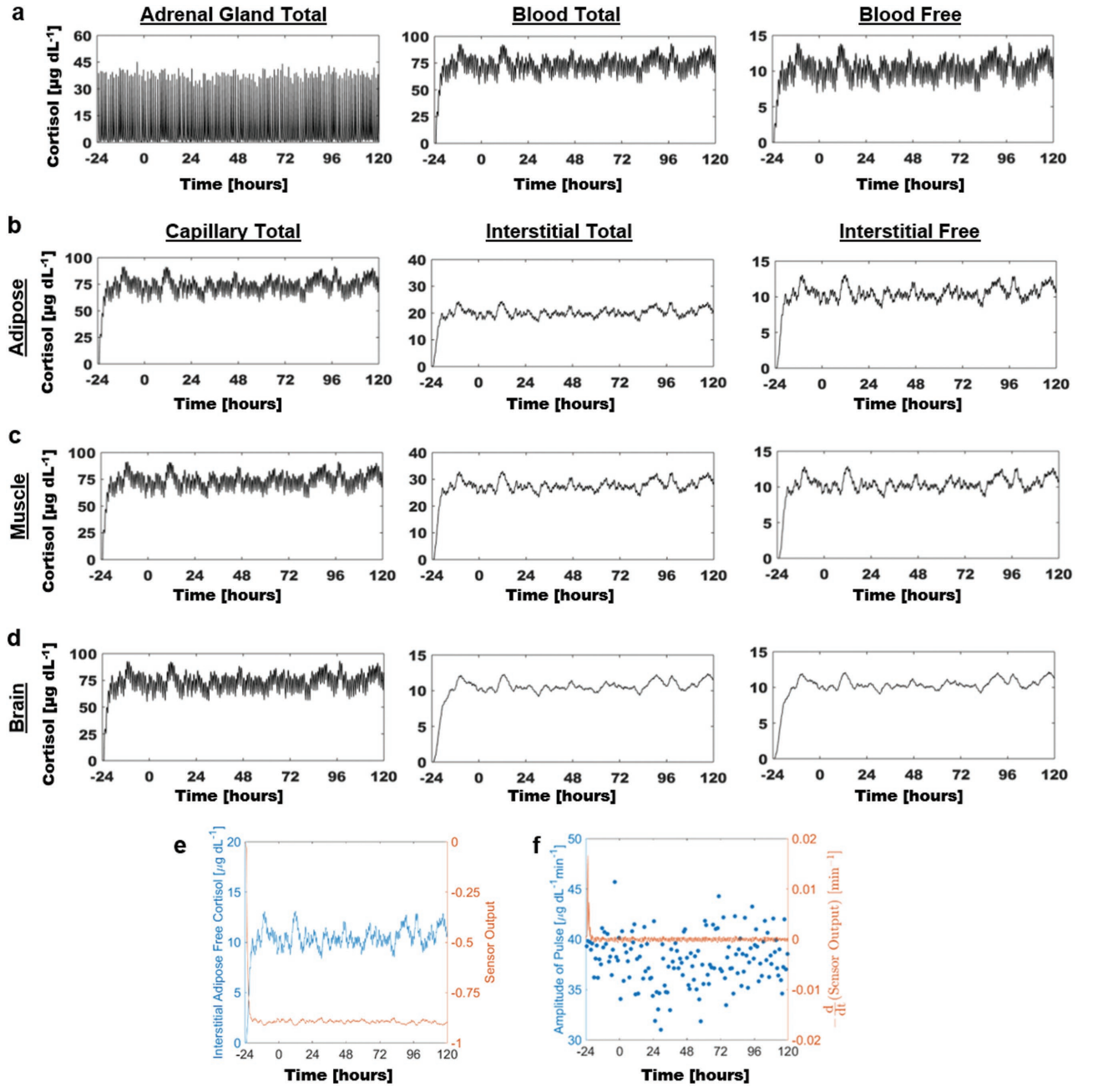

Figure 3. Cortisol concentrations throughout a Cushing's disease patient's body as predicted by the model. Values were calculated in the a) adrenal gland, blood, b) adipose tissue, c) muscle tissue, and d) brain tissue. To obtain similar blood cortisol profiles as the male Cushing's disease patient studied by van den Berg et al.,[61] pulses of 38 ± 2.5 μg dL^{-1} min^{-1} with a 59 ± 11 min waiting time between pulses were introduced into the model. e,f) Sensor output and derivative were also tracked. The sensor showed a flat output relative to that in the normal patient due to the lack of a cortisol diurnal cycle. This output is also close to saturation due to the higher cortisol concentrations.

close in value, such that the sensor respond to both low and high values of cortisol, which is paramount for robustly monitoring the diurnal cycle. When K_D and θ_T have close values, k_b should be as high as possible to maximize sensor output and minimize delay time. Changes in the value of k_b do not change the ratio of the characteristic times of binding and unbinding. Altogether, such a design can provide a robust response to cortisol dynamics while avoiding output saturation, diffusion-limited regimes, and significant delay times in response.

4. Conclusions

In this work, a compartmental model to connect adipose, muscle, and brain tissue cortisol concentrations with blood cortisol concentrations was formulated and verified against reported cortisol measurements. The model was used to calculate cortisol biodistribution in a Cushing's disease patient previously studied by van den Berg et al. and compared against a normal patient's pharmacokinetics.[61] Furthermore, the model

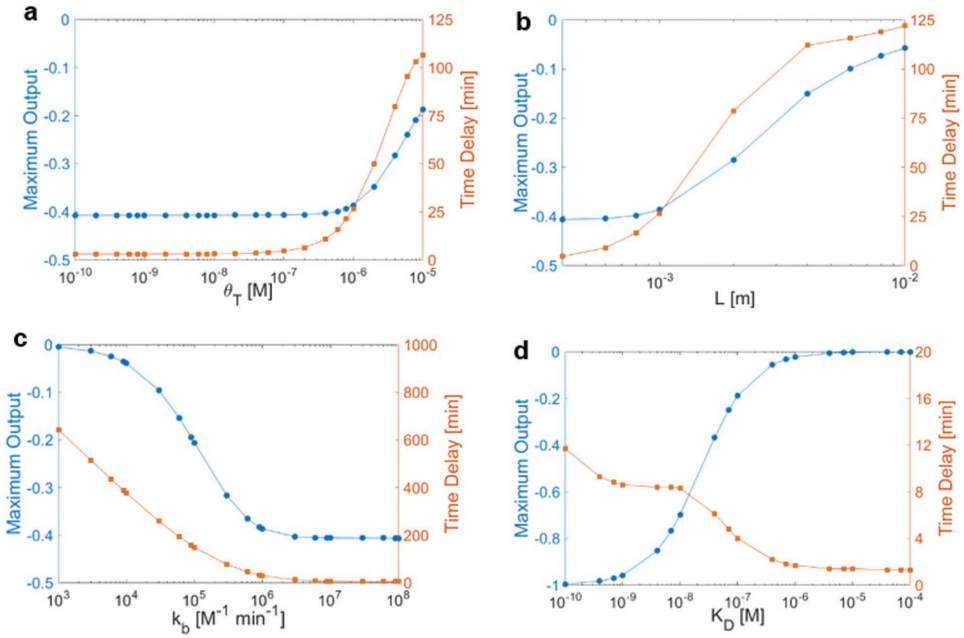

Figure 4. Maximum sensor output and time delay as a function of the a) binding site concentration (θ_T), b) sensor thickness (L), c) forward rate binding constant (k_b), and d) dissociation constant (K_D).

was used to examine a theoretical affinity sensor implanted in the interstitial space of the adipose tissue. Sensor properties, including concentration, geometry, binding kinetics, and binding equilibrium were varied, and their effects on sensor output were calculated to estimate workable parameter values. We conclude that the compartmental representation of the human body is a valuable approach to model cortisol pharmacokinetics and that implantable affinity sensors for continuous cortisol measurements are theoretically possible.

Supporting Information

Supporting Information is available from the Wiley Online Library or from the author.

Acknowledgements

This work was supported by a grant from the Simons Foundation for the Social Brain at MIT. The authors also gratefully acknowledge support from an EAGER grant from the National Science Foundation.

Received: June 19, 2016
Revised: September 1, 2016
Published online:

[1] A. Kaushik, A. Vasudev, S. K. Arya, S. K. Pasha, S. Bhansali, *Biosens. Bioelectron.* **2014**, *53*, 499.
[2] A. Levine, O. Zagoory-Sharon, R. Feldman, J. G. Lewis, A. Weller, *Physiol. Behav.* **2007**, *90*, 43.
[3] T. W. Buchanan, W. R. Lovallo, *Psychoneuroendocrinology* **2001**, *26*, 307.
[4] M. Ebrecht, J. Hextall, L. G. Kirtley, A. Taylor, M. Dyson, J. Weinman, *Psychoneuroendocrinology* **2004**, *29*, 798.
[5] S. T. Yahyavi, M. Zarghami, F. Naghshvar, A. Danesh, *Rev. Bras. Psiquiatr.* **2015**, *37*, 93.
[6] S. K. Gupta, M. P. Dubé, *Clin. Infect. Dis.* **2002**, *35*, E69.
[7] C. Napier, S. H. S. Pearce, *Curr. Opin. Endocrinol., Diabetes Obes.* **2014**, *21*, 147.
[8] R. I. Dorin, H. K. Pai, J. T. Ho, J. G. Lewis, D. J. Torpy, F. K. Urban, C. R. Qualls, *Clin. Biochem.* **2009**, *42*, 64.
[9] G. McCarty, B. Schwartz, *Curr. Eye Res.* **1999**, *18*, 467.
[10] R. T. Faghih, M. A. Dahleh, G. K. Adler, E. B. Klerman, E. N. Brown, *PLoS One* **2014**, *9*, 1.
[11] J. D. Veldhuis, A. Iranmanesh, G. Lizarralde, M. L. Johnson, *Am. J. Physiol.* **1989**, *257*, E6.
[12] R. T. Faghih, K. Savla, M. A. Dahleh, E. N. Brown, *2011 Annu. Int. Conf. IEEE Eng. Med. Biol. Soc.* **2011**, IEEE, Boston, MA, p. 716–719.
[13] J. A. van Heerden, W. F. Young, C. S. Grant, P. C. Carpenter, *Surgery* **1995**, *117*, 466.
[14] L. K. Nieman, *Eur. J. Endocrinol.* **2015**, *173*, M33.
[15] P. Björntorp, R. Rosmond, *Nutrition* **2000**, *16*, 924.
[16] D. S. Sharp, M. E. Andrew, D. B. Fekedulegn, C. M. Burchfiel, J. M. Violanti, J. Wactawski-Wende, D. B. Miller, *Am. J. Hum. Biol.* **2013**, *25*, 499.
[17] H. J. F. Van Marle, E. J. Hermans, S. Qin, S. Overeem, G. Fernández, *Psychoneuroendocrinology* **2013**, *38*, 1639.
[18] J. Gonzalez-Cabrera, M. Fernandez-Prada, C. Iribar-Ibabe, J. M. Peinado, *Stress* **2014**, *17*, 149.
[19] P. Schulz, C. Kirschbaum, J. Prüßner, D. Hellhammer, *Stress Med.* **1998**, *14*, 91.
[20] J. LeMoult, J. Joormann, *Biol. Psychol.* **2014**, *100*, 50.
[21] N. E. Steen, P. Methlie, S. Lorentzen, I. Dieset, M. Aas, M. Nerhus, M. Haram, I. Agartz, I. Melle, J. P. Berg, O. A. Andreassen, *J. Psychiatr. Res.* **2014**, *52*, 57.
[22] R. Gatti, G. Antonelli, M. Prearo, P. Spinella, E. Cappellin, E. F. De Palo, *Clin. Biochem.* **2009**, *42*, 1205.
[23] G. Montskó, Z. Tarjányi, E. Mezősi, G. L. Kovács, *Anal. Bioanal. Chem.* **2014**, *406*, 2333.
[24] R. Faghih, M. Dahleh, G. Adler, E. Klerman, E. Brown, *IEEE Trans. Biomed. Eng.* **2015**, *9294*, 1.

[25] T. Carroll, H. Raff, J. W. Findling, *Nat. Clin. Pract. Endocrinol. Metab.* **2008**, *4*, 344.
[26] M. J. Sheriff, B. Dantzer, B. Delehanty, R. Palme, R. Boonstra, *Oecologia* **2011**, *166*, 869.
[27] C. A. Manire, L. E. L. Rasmussen, K. P. Maruska, T. C. Tricas, *Comp. Biochem. Phsyiol.* **2007**, *148*, 926.
[28] M. Venugopal, S. K. Arya, G. Chornokur, S. Bhansali, *Sens. Actuators, A: Phys.* **2011**, *172*, 154.
[29] R. C. Bhake, J. A. Leendertz, A. C. E. Linthorst, S. L. Lightman, *J. Med. Eng. Technol.* **2013**, *37*, 180.
[30] N. M. Iverson, G. Bisker, E. Farias, V. Ivanov, J. Ahn, G. N. Wogan, M. S. Strano, *J. Biomed. Nanotechnol.* **2016**, *12*, 1035.
[31] M. P. Landry, S. Kruss, J. T. Nelson, G. Bisker, N. M. Iverson, N. Reuel, M. Strano, *Sensors* **2014**, *14*, 16196.
[32] J. Zhang, M. P. Landry, P. W. Barone, J.-H. Kim, S. Lin, Z. W. Ulissi, D. Lin, B. Mu, A. A. Boghossian, A. J. Hilmer, A. Rwei, A. C. Hinckley, S. Kruss, M. A. Shandell, N. Nair, S. Blake, F. Őren, S. Őren, R. G. Croy, D. Li, K. Yum, J.-H. Ahn, H. Jin, D. A. Heller, J. M. Essigmann, D. Blankschtein, M. S. Strano, *Nat. Nanotechnol.* **2013**, *8*, 959.
[33] N. M. Iverson, P. W. Barone, M. Shandell, L. J. Trudel, S. Sen, F. Sen, V. Ivanov, E. Atolia, E. Farias, T. P. McNicholas, N. Reuel, N. M. A. Parry, G. N. Wogan, M. S. Strano, *Nat. Nanotechnol.* **2013**, *8*, 873.
[34] S. Kruss, M. P. Landry, E. Vander Ende, B. M. A. Lima, N. F. Reuel, J. Zhang, J. Nelson, B. Mu, A. Hilmer, M. Strano, *J. Am. Chem. Soc.* **2014**, *136*, 713.
[35] G. Bisker, J. Dong, H. D. Park, N. M. Iverson, J. Ahn, J. T. Nelson, M. P. Landry, S. Kruss, M. S. Strano, *Nat. Commun.* **2016**, *7*, 10241.
[36] B. Mu, J. Ahn, T. P. McNicholas, M. S. Strano, *Chem. – Eur. J.* **2015**, *21*, 4523.
[37] E. N. Brown, P. M. Meehan, A. P. Dempster, *Am. J. Physiol.: Endocrinol. Metab.* **2001**, *280*, E450.
[38] S. A. Glantz, J. A. Luetscher, R. P. Day, M. Perloff, *IEEE Trans. Biomed. Eng.* **1976**, BME-*23*, 36.
[39] M. N. Smith, W. C. Griffith, S. A. A. Beresford, M. Vredevoogd, E. M. Vigoren, E. M. Faustman, *J. Exposure Sci. Environ. Epidemiol.* **2013**, *24*, 510.
[40] J. T. Sorensen, *Ph.D. Thesis*, MIT **1985**.
[41] G. Bisker, N. M. Iverson, J. Ahn, M. S. Strano, *Adv. Healthcare Mater.* **2015**, *4*, 87.
[42] G. S. Rao, K. Schulze-Hagen, M. L. Rao, H. Breuer, *J. Steroid Biochem.* **1976**, *7*, 1123.
[43] G. S. Rao, *Mol. Cell. Endocrinol.* **1981**, *21*, 97.
[44] N. C. Lan, M. Karin, T. Nguyen, A. Weisz, M. J. Birnbaum, N. L. Eberhardt, J. D. Baxter, *J. Steroid Biochem.* **1984**, *20*, 77.
[45] R. H. Stimson, J. Andersson, R. Andrew, D. N. Redhead, F. Karpe, P. C. Hayes, T. Olsson, B. R. Walker, *Diabetes* **2009**, *58*, 46.
[46] I. Oren, S. J. Fleishman, A. Kessel, N. Ben-Tal, *Biophys. J.* **2004**, *87*, 768.
[47] G. Bleau, K. D. Roberts, A. Chapdelaine, *J. Clin. Endocrinol. Metab.* **1974**, *39*, 236.
[48] I. Gersh, M. A. Still, *J. Exp. Med.* **1945**, *81*, 219.
[49] S. R. Ward, R. L. Lieber, *J. Biomech.* **2005**, *38*, 2317.
[50] R. Myrhage, O. Hudlická, *Microvasc. Res.* **1976**, *11*, 315.
[51] M. Ellmerer, L. Schaupp, G. A. Brunner, G. Sendlhofer, A. Wutte, P. Wach, T. R. Pieber, *Am. J. Physiol.: Endocrinol. Metab.* **2000**, *278*, E352.
[52] S. Schwarz, P. Pohl, *Neuroendocrinology* **1992**, *55*, 174.
[53] A. Munck, N. J. Holbrook, *J. Biol. Chem.* **1984**, *259*, 820.
[54] J. Cohen, R. Deans, A. Dalley, J. Lipman, M. S. Roberts, B. Venkatesh, *Crit. Care* **2009**, *13*, R189.
[55] A. Mehta, R. R. Mahale, U. Sudhir, M. Javali, R. Srinivasa, *Ann. Indian Acad. Neurol.* **2015**, *18*, 210.
[56] M. Holub, O. Beran, O. Dzupová, J. Hnyková, Z. Lacinová, J. Príhodová, B. Procházka, M. Helcl, *Crit. Care* **2007**, *11*, R41.
[57] M. Santarsieri, C. Niyonkuru, E. H. McCullough, J. A. Dobos, C. E. Dixon, S. L. Berga, A. K. Wagner, *J. Neurotrauma* **2014**, *31*, 699.
[58] M. Gordic, *Master's Thesis*, University of South Florida **2008**.
[59] E. Delaney, *The Relationship Between Traumatic Stress, PTSD, and Cortisol, Nav. Cent. Combat Oper.*Stress Control, San Diego, CA, **2013**.
[60] P. Linkowski, J. Mendlewicz, R. Leclercq, M. Brasseur, P. Hubain, J. Golstein, G. Copinschi, E. Van Cauter, *J. Clin. Endocrinol. Metab.* **1985**, *61*, 429.
[61] G. van den Berg, M. Frolich, J. D. Veldhuis, F. Roelfsema, *J. Clin. Endocrinol. Metab.* **1995**, *80*, 3750.

Adv. Healthcare Mater. **2016**,
DOI: 10.1002/adhm.201600650